Research Article

# Tribological performances of hexagonal boron nitride nanosheets via surface modification with silane coupling agent

Lixia Wang[1,2] · Yufeng Bai[1] · Zhiyan Ma[1,3] · Chunhua Ge[1] · Hongyu Guan[1] · XiangDong Zhang[1]

## Abstract

Hexagonal boron nitride (h-BN) is a promising lubricant additive for decreasing wear and friction. However, the poor dispersion stability and bulky size of h-BN restricted its lubrication application. In this paper, bulk h-BN was exfoliated into h-BN nanosheets (h-BNNSs), and then the self-made h-BNNSs were chemically modified with silane coupling agent via a facile and scalable reaction method. The morphology and structure of surface-functionalized h-BNNSs (m-BNNSs) were certified using a series of characterizations. Results revealed that h-BNNSs could be chemically well capped by surface modifier and the lipophilic groups were covalently attached to h-BNNSs surfaces. The m-BNNSs composite possessed long-term dispersion in liquid paraffin (LP). At the optimal adding content of 0.6 wt%, coefficient of friction and wear volume of m-BNNSs composite were decreased by about 31.9% and 53.8% compared with those of LP, respectively. Therefore, m-BNNSs composite as a lubricating oil additive has high research value and good prospects of lubrication applications.

## 1 Introduction

Two-dimensional hexagonal boron nitride (h-BN) has gained tremendous attention due to its profound mechanical strength, remarkable oxidation resistance, and unique atom-thick structure, etc. [1–3]. In recent years, h-BN has been widely used in many fields, such as electronic devices [4, 5], pollutant adsorption [6, 7], composite materials [8, 9], lubricity [10–12] and so on. Among them, the lubrication application of h-BN has allured lots of interests because this material has been confirmed as a promising lubricant additive for decreasing wear and friction. Many studies have been conducted on h-BN particles with different size and morphology as solid additives to oil lubricants. Menezes et al. [13] investigated the effects of h-BN particles with varying sizes on lubrication performances of the avocado oil. The results indicated that nano-sized h-BN particles have the lowest friction and wear values compared with micron-sized and submicron-sized h-BN particles. Shtansky et al. [14] synthesized three different morphologies h-BN nanoparticles (hollow particles, solid particles, and globular particles) and found that the presence of three shapes nanoparticles in Polyalphaolefin-6 (PAO6) oil has antifriction and anti-wear effects. Of all the three additives, globular particles formed by many thin h-BNNSs perform best on tribological properties. Under the condition of boundary lubrication, the roughness of worn surface directly contacts with each other. To reduce wear and friction of the relative contact surface, the additive particles must enter the friction interfaces. Therefore, the thickness of bulk h-BN material can be reduced to make it easy to enter the contact surface.

✉ Chunhua Ge, chhge@lnu.edu.cn; ✉ XiangDong Zhang, xd623@sina.com | ¹College of Chemistry, Liaoning University, Liaoning Province 110036, Shenyang, People's Republic of China. ²Siziwang Banner Branch, Wulanchabu Municipal Bureau of Ecology and Environment, Inner Mongolia Autonomous Region, Wulanchabu 011800, People's Republic of China. ³Department of Chemical and Environmental Engineering, Yingkou Institute of Technology, Liaoning Province 115014, Yingkou, People's Republic of China.

At present, a common approach to change the bulky size of h-BN is to peel it into h-BN nanosheets. As an important member of h-BN materials, the h-BNNSs have unique characteristics in comparison to bulk h-BN counterparts, such as its high specific surface areas, profound mechanical strength, and robust lubricity [15–17]. Very recent research shows that the exfoliating their bulk forms into few layers or monolayer of h-BNNSs can significantly improve the tribological behaviors of h-BN particles [18, 19]. Sahu et al. [20] reported that oxygen functionalized h-BNNSs were produced by exfoliation of the bulk h-BN powders via ball milling and ultrasonic technique. Results indicated that a small amount of oxygen functionalized h-BNNSs in lubricating oil has excellent lubricating capabilities. Ma et al. [21] exfoliated the bulk h-BN powders to 2–3 layered h-BNNSs through hydrothermal treatment and sonication processes, and they discovered that few-layered h-BNNSs had good friction-reducing ability and wear resistance. Ahmad et al. synthesized high quality boron nitride nanotubes via Argon supported thermal chemical vapor deposition at a relatively lower temperature of 900 °C [22]. As known to all, the dispersion stability of h-BNNSs-based materials in lubricating oil can determine their friction and wear performance to a certain extent. However, h-BNNSs is incompatible with the lube media. Because of the interactions of van der Waals, the exfoliated nanosheets may deposit and re-accumulate. Thus, the functionalization of h-BNNSs by surface modifier is needed to improve its compatibility with base oil. Wang et al. [23] found that h-BN nanoparticles modified by silane coupling agent had better lipophilicity and dispersion than unmodified nanoparticles because of the lipophilic groups attached to their surface. When incorporated into castor oil, the modified h-BN nanoparticles exhibited excellent lubrication properties. To date, numerous studies have shown that the chemical modification of h-BNNSs surface is an effective method to improve its compatibility and dispersion [24, 25]. As we all know, the silane coupling agent is a commonly used surface modifier [26]. In fact, the functionalization of chemically inert h-BNNSs is primarily achieved through the reaction of the modifier with the surface-active groups of h-BNNSs. The active groups,

such as hydroxide groups, play a major role in the modification on h-BNNSs surfaces. Unfortunately, the surface of h-BNNSs possesses very few functional groups [27]. To overcome the inert problem of h-BNNSs, it is necessary to introduce hydroxide groups on the h-BNNSs surfaces, which will expand its application fields.

Previously, our group has explored the performance of boron nitride materials as water-based and oil-based lubricating additives [25, 28, 29]. However, the preparation process of boron nitride as an oil-based lubricant additive is relatively complex. In this study, the oil-based boron nitride additive was prepared by a simple method. h-BNNSs were exfoliated from bulk h-BN via molten alkali hydroxides pretreatment and sonication, and the surface of h-BNNSs was hydroxylated with strong alkali to enhance the combination of h-BNNSs and surface modifier. Then, the hydroxylated h-BNNSs were covalently functionalized by 3-(Trimethoxysilyl)propyl methacrylate (KH570) to produce m-BNNSs composite. The synthetic routes of m-BNNSs are shown in Fig. 1. The dispersing performance and tribological properties of the obtained h-BNNSs and m-BNNSs in LP were evaluated.

## 2 Experimental

### 2.1 Materials

Hexagonal boron nitride was received from Dandong Rijin Science and Technology Co. Ltd. (Shenyang, China). 3-(Trimethoxysilyl)propyl methacrylate was supplied by Sinopharm Chemical Reagent Co. Ltd. (Shanghai, China). Potassium hydroxide, sodium hydroxide, and hydrochloric acid were received from Shanghai Jingchun Industrial Co. Ltd. (Shanghai, China), and it was used without further purification.

### 2.2 Synthesis of h-BNNSs composite

The as-exfoliated h-BNNSs were obtained through the molten alkali hydroxide-assisted liquid exfoliation method as described in our previous work [28]. Because of the
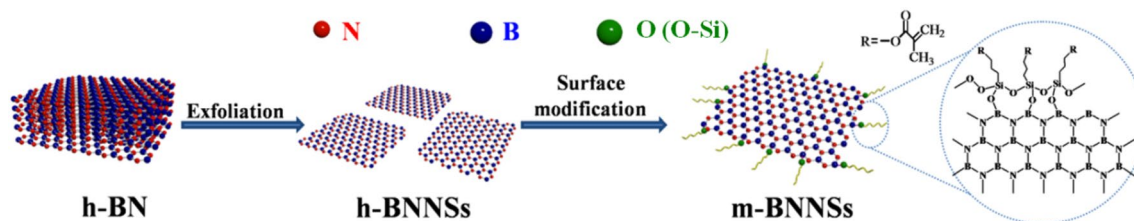


**Fig. 1** Schematic of the synthesis routes of m-BNNSs

lack of active functional groups on the h-BNNSs surface, h-BNNSs can not be effectually modified by KH570. Therefore, in order to expand the application prospect of h-BN, h-BN is generally used after being functionalized [25]. The hydroxylation of h-BNNSs is obtained by reaction with hot sodium hydroxide solution, as described in our previous work [30]. The regained product was denoted as hydroxyl-functionalized h-BNNSs. Then, a certain amount of KH570 (5 wt% of the mass of hydroxyl-functionalized h-BNNSs) dissolved in a 95:5 mixture of absolute ethanol and ultrapure water by stirring for 1 h, adjusting the pH of the ethanol aqueous solution to 3–5 using $CH_3COOH$ and hydrolyzing for 30 min. After this, quantitative hydroxyl-functionalized h-BNNSs were added to the above mixture and ultrasonic for 1 h. The mixture was stirred at 80 °C for 6 h and then stood for 2 h. At this time, KH570 molecules are primarily physically absorbed on the h-BNNSs surfaces via hydrogen bonds, and the obtained powders were denoted as h-BNNSs + KH570. To form covalent bonds between the silane coupler KH570 and h-BNNSs, the mixture was thermally treated at 110 °C for 10 h. After the reaction ended, the resultant product was rinsed with absolute ethanol at least three times to remove the unreacted KH570 and other impurities without grafting, and then dried. The surface functionalized h-BNNSs composite was obtained and coded as m-BNNSs. The yield of m-BNNSs is not higher than 10%.

## 2.3 Characterizations

Fourier-transform infrared spectroscopy (FT-IR, Nicolet AVATAR 360) was utilized to measure whether h-BNNSs was successfully exfoliated and KH570 was grafted onto the h-BNNSs surface. The microstructure and morphology of bulk h-BN, h-BNNSs, and m-BNNSs were identified by X-ray diffraction patterns (XRD, Bruker D8, Cu Kα radiation, λ = 0.15406 nm), Raman spectra (Jobin–Yvon T64000) and scanning electron microscope images (SEM, FEI QUANTA200). Thermo-gravimetric analysis (TGA) curve of as-prepared sample was obtained utilizing a METTLER SDTA-851e thermal tester. The UV–Vis spectrum was examined using a Shimadzu UV-3150.

## 2.4 Tribological tests

The bulk h-BN, as-exfoliated h-BNNSs or as-prepared m-BNNSs were dispersed in LP by sonication for 1 h to form uniform dispersion with different mass fractions. The added contents of h-BN, h-BNNSs and m-BNNSs were 0.2, 0.4, 0.6, 0.8 and 1.0 wt%, respectively. The tribological properties of pure LP and LP containing h-BN, h-BNNSs and m-BNNSs were conducted through measuring wear and friction using an MMW-1A four-ball tester (Jinan Yihua

Tribology Tester Technology Co. Ltd.). The operating conditions for the tests were under the applied load of 294 N and the rotary speed of 1450 rpm, and the testing time was 60 min. GCr15 bearing steel balls (12.7 mm) were used for tribological measurement and cleaned with petroleum ether before starting each experiment. The wear performance was evaluated by the wear scar of the lower balls which was examined under YW MS2300D optical microscope. In order to gain average friction coefficient (COF) and wear scar diameter (WSD) values, three repeated tribological experiments were carried out on each sample. Furthermore, mean wear volume (MWV) was calculated from following Eqs. (1) and (2) [31]:

$$h = r - \sqrt{r^2 - \frac{d^2}{4}} \qquad (1)$$

$$MWV = \frac{\pi h}{6}\left(\frac{3d^2}{4} + h^2\right) \qquad (2)$$

where $d$ is WSD (mm) and r is the radius of the ball (mm).

## 3 Results and discussion

As described by Fig. 1, h-BNNSs were prepared via exfoliating the bulk h-BN powder, and then h-BNNSs were surface functional modified with KH570 to produce m-BNNSs. It is the fact that successful exfoliating of h-BNNSs and grafting of KH570 on h-BNNSs are confirmed by FT-IR spectrum, Raman spectrum, XRD pattern, and TGA curve. Figure 2a displays the FT-IR spectra of commercial bulk h-BN, h-BNNSs, and m-BNNSs. Two sharp absorption peaks at 1375 $cm^{-1}$ and 815 $cm^{-1}$ in the spectra of h-BN and h-BNNSs correspond to B-N in-plane stretching vibration and B-N out-of-plane bending vibration, respectively [32]. In comparison with h-BN, the peak at about 1375 $cm^{-1}$ is significantly broadened in the h-BNNSs spectra, denoting h-BNNSs is partially hydroxylated [33]. After grafting of KH570, many new adsorption peaks of KH570 can be observed in m-BNNSs. The additional peaks at 2947 $cm^{-1}$ and 2841 $cm^{-1}$ are features of the C–H stretching of $-CH_3$ and $-CH_2-$ groups [26]. The appearance of the peak at 1732 $cm^{-1}$ is assigned to the C = O stretching vibration from the grafted KH570. Moreover, the Si–C stretching vibration is represented by the characteristic peaks at 784 $cm^{-1}$ and 820 $cm^{-1}$, and in the range of 925–1195 $cm^{-1}$ is designated as the Si–O stretching vibration [34]. The FT-IR analysis results illustrate that the surface of h-BNNSs has successfully functionalized by KH570 in a non-covalent manner to generate m-BNNSs.

**Fig. 2** FT-IR spectra (**a**), XRD (**b**), Raman spectra (**c**), TGA (**d**) and the thermal weightlessness of pristine bulk h-BN, h-BNNSs and m-BNNSs
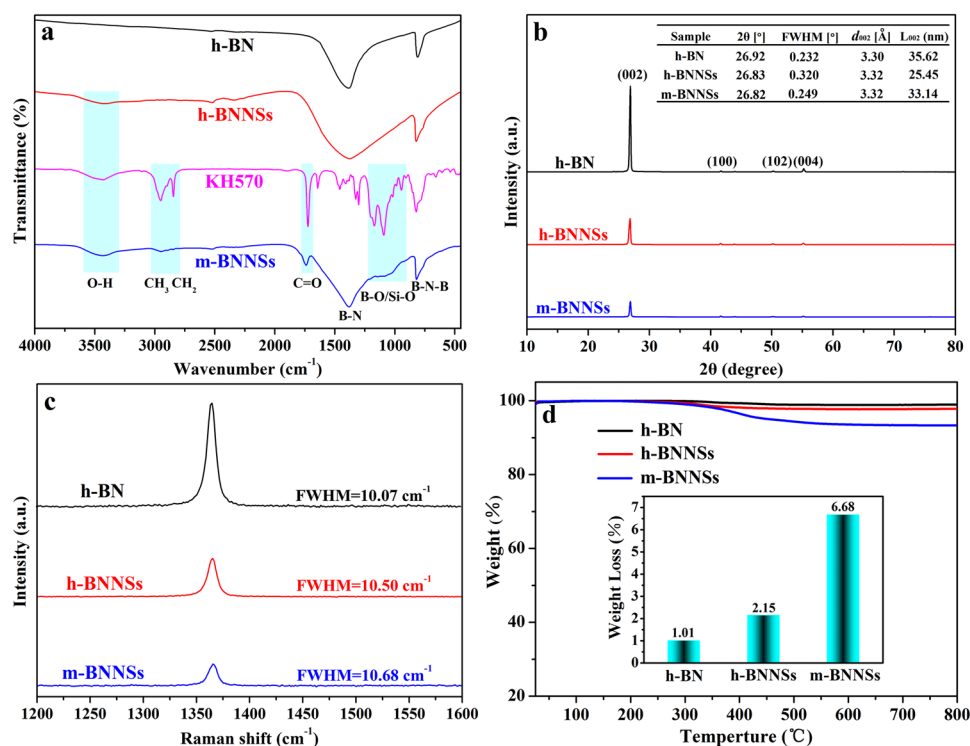


As displayed in the XRD patterns (Fig. 2b), h-BN, h-BNNSs and m-BNNSs have four similar diffraction peaks at about $2\theta = 26.9°$, $41.6°$, $50.2°$ and $55.2°$, which can be indexed to (002), (100), (102) and (004) planes (JCPDS card no. 34–0421), respectively. Compared with h-BN, no diffraction peak of other crystal phases is found in h-BNNSs and m-BNNSs. However, the peak intensities of h-BNNSs and m-BNNSs are weaker than h-BN, especially (002) peak. The weakening of peaks intensity means that the structural order of h-BNNSs and m-BNNSs is significantly decreased, which demonstrates that h-BNNSs and m-BNNSs have few layers, and the accumulation of the c-direction is weaker than bulk h-BN [35]. This phenomenon also confirmed through the change of interlayer distance ($d_{002}$) and thickness ($L_{002}$) of h-BNNSs and m-BNNSs in the table inserted in Fig. 2b. Comparing to h-BN, the $d_{002}$ of h-BNNSs and m-BNNSs increases, and the $L_{002}$ decreases. In addition, the (002) peak of h-BNNSs and m-BNNSs appears to shift slightly from $26.92°$ (h-BN) to $26.83°$ and $26.82°$, which are related to the increase of the interlayer distance from 3.30 (h-BN) to 3.32 and 3.32 Å, respectively. Clearly, the exfoliation and surface modification of h-BNNSs will not damage or change the crystal structure of h-BN matrix.

The h-BN, h-BNNSs, and m-BNNSs are further analyzed by Raman spectra, as presented in Fig. 2c. In Raman spectra of h-BN, h-BNNSs and m-BNNSs, a typical peak of the lamellar h-BN structure at about 1366 cm$^{-1}$ is observed which belongs to $E_{2g}$ vibration mode [36]. In comparison with commercial h-BN, the intensity of $E_{2g}$ vibration mode

for h-BNNSs shows a decrease. This phenomenon has been thoroughly studied in previous report [37]. After surface modification of KH570, the peak intensity of m-BNNSs decreases significantly, indicating that KH570 has been successfully attached to the surface of h-BNNSs. Besides, the full-width at half-maximum (FWHM) of the $E_{2g}$ mode is measured to provide further information on the characteristics of bulk h-BN, h-BNNSs, and m-BNNSs composite. The FWHM of h-BNNSs and m-BNNSs is estimated as 10.50 cm$^{-1}$ and 10.68 cm$^{-1}$, slightly larger than bulk h-BN (10.07 cm$^{-1}$). This smaller broadening of the $E_{2g}$ vibration peak may be caused by lower defects. These phenomena are in accordance with the previous reports [29, 30].

TGA is applied to analyze the thermal stability of h-BNNSs and m-BNNSs (Fig. 2d). As a comparison, the TGA curve of commercial h-BN is also tested. As expected, the TGA curve for bulk h-BN has little change in weight below 800 °C, indicating that it has high thermal stability. The weight loss of h-BNNSs is apparent (about 2.15%), which is ascribed to the existence of hydroxyl groups [33]. By comparing thermal weight loss of h-BNNSs and m-BNNSs, the amount of KH570 in m-BNNSs is estimated to be approximately 4.53%, which is related to the functional reaction of h-BNNSs with KH570 and bring about some attachment of siloxane onto the surface of h-BNNSs. The above result further indicates the covalent grafting of KH570 to h-BNNSs.

SEM is carried out to further study the morphology of bulk h-BN, h-BNNSs, and m-BNNSs, and the results are given in Fig. 3. The h-BN powder presents the opaque

**Fig. 3** SEM micrographs of the initial bulk h-BN (**a–b**), h-BNNSs (**c–d**), and m-BNNSs (**e–f**) at low magnification and high magnification
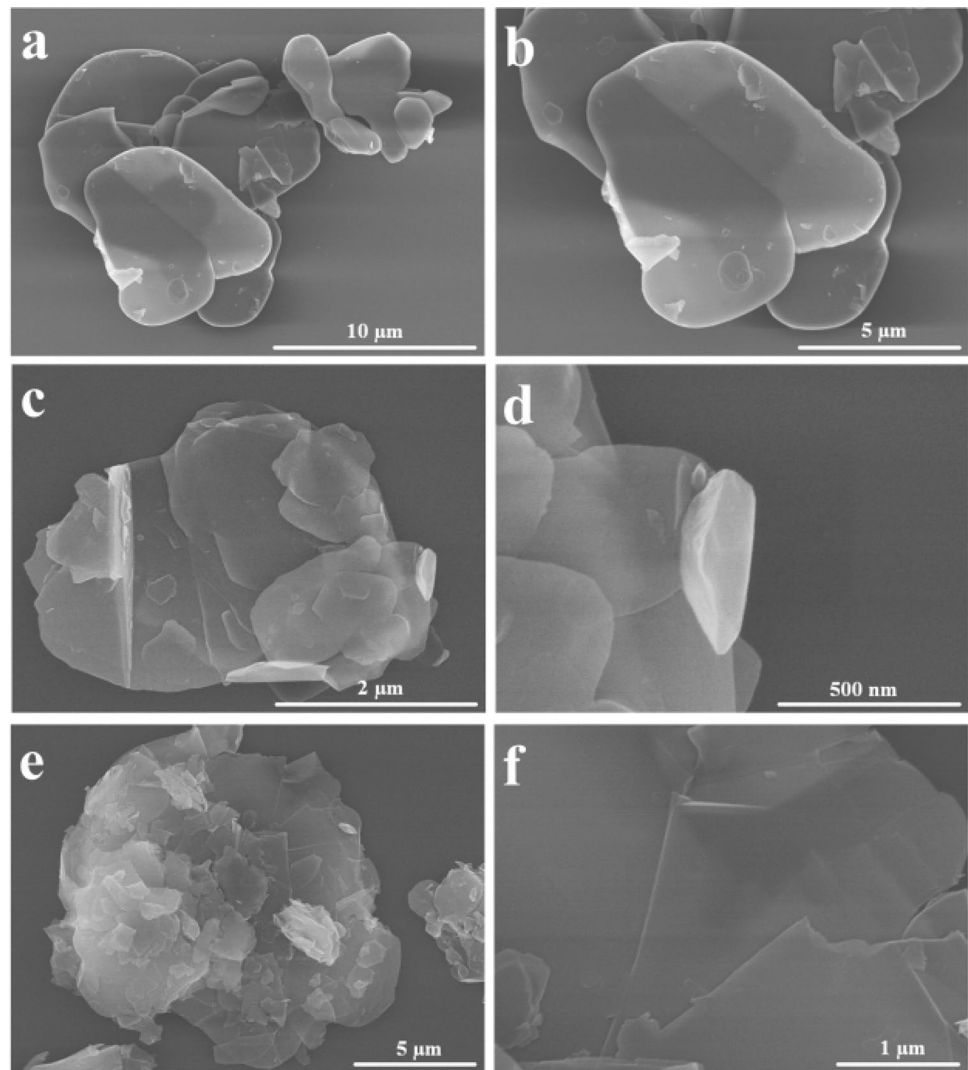


bulk-like structure and irregular shapes (Fig. 3a and b) [28]. Comparatively, the morphologies of h-BNNSs (Fig. 3c and d) and m-BNNSs (Fig. 3e and f) are different from their bulk counterparts. After the exfoliation process, a large number of h-BN nanosheets are found in Fig. 3c and d. It shows a clear layered structure composed of the randomly stacked irregular nanosheets. Compared with h-BN, the thickness of h-BNNSs is significantly reduced and nearly transparent. This result demonstrates that bulk h-BN is exfoliated into mono-layer or few layers [38, 39]. As seen in Fig. 3e and f, the m-BNNSs composite also shows larger fragments and the lamellar structures, determined by the structure of h-BNNSs. Furthermore, the m-BNNSs composite presents disordered secondary aggregates composed of primarily many nanosheets, which will play an essential role in lubrication.

The dispersion stability of h-BNNSs-based materials can determine their friction and wear capability to a certain extent [12]. For tribological application, it is essential to evaluate the dispersion of m-BNNSs as LP additive. Hence, the dispersion of h-BN, h-BNNSs and m-BNNSs in LP depending on the time is explored. The h-BN, h-BNNSs, and m-BNNSs are added into LP and then dispersed thoroughly through sonication to obtain homogeneous dispersions with a mass fraction of 0.6 wt%. As illustrated in Fig. 4a, the relative absorbance of h-BN, h-BNNSs, and m-BNNSs dispersions gradually decreases with the increase of the settling time. What's more surprising is that the stability of three additives is a significant difference. The h-BN dispersion has a serious sedimentation phenomenon, and the settling velocity is the fastest, which is ascribed to the agglomeration. The h-BNNSs and m-BNNSs dispersions are adequately stable, indicating that h-BNNSs and m-BNNSs have better dispersion stability in LP than h-BN. After standing for 7 days, m-BNNSs dispersion possesses maximum stability in LP. The result demonstrates that KH570 successfully improves the dispersion stability of h-BNNSs. The possible reason for this

**Fig. 4** (**a**) UV spectra and the dispersed photographs at different settling times of LP, 0.6 wt% h-BN, h-BNNSs, and m-BNNSs. (**b**) The absorbance of m-BNNSs at different settling times
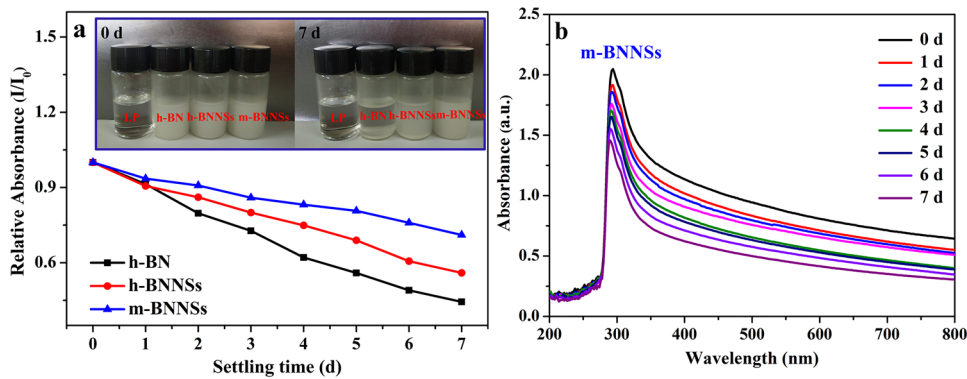
phenomenon is the introduction of lipophilic groups in m-BNNSs, which enhances the dispersion and compatibility of the additive in LP. For the sake of brevity, Fig. 4b shows only the absorbance of 0.6 wt% m-BNNSs as an LP additive at different settling times. It is apparent that the m-BNNSs dispersion absorbs at about 290 nm and the absorbance decreases from around 2.048 to 1.456 within 7 days. These phenomena are in accordance with the previous reports [28]. The inserted photographs in Fig. 4a compares the dispersion stability of LP containing 0.6 wt% h-BN, h-BNNSs, and m-BNNSs at different storage times. It can be seen from the figure that the exfoliated h-BNNSs and as-modified m-BNNSs are of excellent dispersion stability. More surprisingly, the commercial bulk h-BN powders fully sediment after seven days. With the increase of time, the h-BNNSs is easy to precipitate. When the h-BNNSs dispersion was places for seven days, the deposition can be seen. It is worth to mention that the m-BNNSs can be stably dispersed in LP until seven days, which indicates its great potential to be applied as an oil-based additive for lubrication. In addition, compared with the previous work, the composite material shows better settlement stability [21, 29].

The tribological performances are closely associated with the concentration of the lubricating oil additives, so the additive concentration must be optimized before the tribological tests. To explore the effect of the concentration of h-BN, h-BNNSs, and m-BNNSs on antifriction performance of LP, the COFs of LP containing 0.2 wt%, 0.4 wt%, 0.6 wt%, 0.8 wt% and 1.0 wt% of three additives are investigated, as presented in Fig. 5a. It can be seen that the average COFs of three additives in LP are smaller than those of LP without any additives at all the concentrations. This result illustrates that three additives are capable of improving the antifriction property of LP, which is attributed to the inherent lubrication capabilities of two-dimensional layered materials [35]. The h-BNNSs, and m-BNNSs performs better on friction-reducing property in comparison with h-BN. The mechanism of good lubrication ability is because of the interactions of weak van der Waals between the loosely packed h-BN nanosheets, which promotes inter-plane sliding, thus reducing the friction between the balls and balls [40]. When m-BNNSs is added to LP for friction, the weak interlayer interactions of m-BNNSs are conducive to the shear of nanosheets on sliding interfaces, which significantly improve lubricating properties. When the concentration of the h-BN increases from 0.2 to 0.6 wt%, the average COFs decrease gradually. A further reduction in the average COFs value is observed when h-BNNSs and m-BNNSs are subsequently used. Compared to the h-BNNSs, the maximum decrease is visible for m-BNNSs. The reason for this phenomenon is due to the fact that the m-BNNSs has agglomerated (Fig. 3e) and they may have been separated during friction. As a result



**Fig. 5** (**a**) Variation of average COF with different concentrations. (**b**) The COF curves of pure LP, 0.6 wt% h-BN, h-BNNSs, and m-BNNSs dispersions
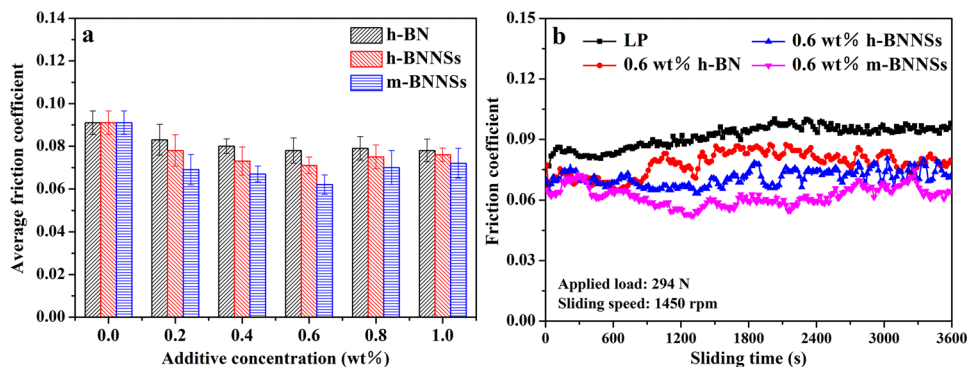
of this the COF value is decreased. However, the average COFs significant increase when the h-BN, h-BNNSs, and m-BNNSs concentrations exceed 0.6 wt%. These results manifest that under the same conditions, the addition of 0.6 wt% three additives display superior friction-reducing property. Therefore, 0.6 wt% can be considered as the optimal concentration of three additives in LP. This appropriate concentration can make h-BN, h-BNNSs, and m-BNNSs deposit on the steel balls more evenly, and support the sliding contact surfaces more effectively.

Figure 5b displays the variation in COF of LP, 0.6 wt% h-BN, h-BNNSs, and m-BNNSs dispersions. The COF values of LP are always higher than three additives during the whole friction stage, indicating that three additives have excellent friction-reducing property. In the starting stage, the COF curves of LP and three additives appear a remarkably upward trend. This phenomenon is because the temperature of the contacting interfaces rises rapidly under the action of intense friction, which intensifies the thermal movement of three additives and LP adsorbed on the contact interfaces, increasing the friction inside the adsorption films, thereby increasing the COF. As the friction continues, the COF of LP increases gradually and then tends to be stable at a high value. In the presence of h-BN, the COF values instantly decline, and then a noticeable rise in the COF values is observed with the increase of friction time. This is probably because of the severe agglomeration of the bulk h-BN in LP, resulting in unstable protective films on friction pair surfaces. When adding 0.6 wt% h-BNNSs and m-BNNSs, the COF values are further reduced. For h-BNNSs, the curve fluctuates continuously after sliding for 1800s. This result indicates that h-BNNSs can form effective protective films on the friction surfaces at the initial stage. However, h-BNNSs has relatively poor dispersion stability in LP, and there will be slight agglomeration as sliding continues, which will disturbs its continuous contact on the surface. In comparison, the COF of the 0.6 wt% m-BNNSs is much lower than that of h-BNNSs during the test duration, meaning that m-BNNSs has superior friction reduction ability. Obviously, the average COF value of 0.6 wt% m-BNNSs dispersion is reduced by 31.9% relative to LP alone. This is probably because the m-BNNSs composite adsorbs on the rubbing surfaces to form more compact and stable protective tribo-films, and the tribo-films are not easy to be destroyed.

Figure 6 presents the average WSD and MWV of LP and 0.6 wt% h-BN, h-BNNSs, and m-BNNSs. As seen in the figure, three additives have a smaller average WSD than pure LP, demonstrating that three additives are useful for improving the anti-wear performance of LP. This may be because the three additives pone to enter and deposit on sliding interfaces, avoiding the direct contact of the friction surface. Furthermore, the h-BNNSs and m-BNNSs have
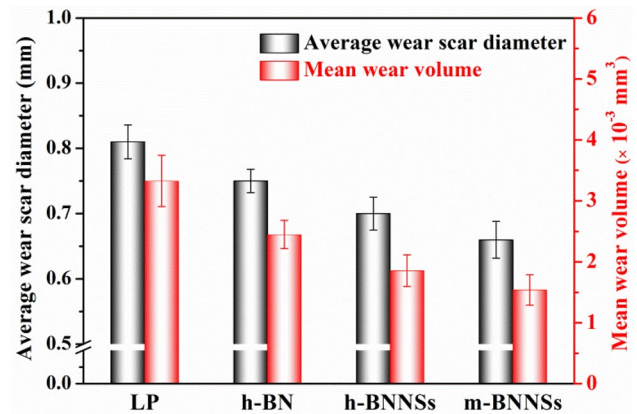


**Fig. 6** Comparison the average WSD and corresponding MWV of the lower ball using LP, 0.6 wt% h-BN, h-BNNSs and m-BNNSs throughout friction test

better wear resistance. Compared to h-BN, the h-BNNSs and m-BNNSs as LP additives can increase the area of contact between friction pairs and lubricant, and they play a role of protective layers, thereby effectively reducing wear [41]. Among them, m-BNNSs exhibits a superior wear-resistance property compared to the other two additives. The WSD of m-BNNSs is 0.66 mm, which is 18.5% less than that of the LP (0.81 mm). The rule of wear behavior for three additives is similar to that for the antifriction property. Thus, m-BNNSs composite is more suitable as antifriction and anti-wear additives of LP.

To further evaluate wear performance of three additives, the MWV of the steel balls lubricated by LP, 0.6 wt% h-BN, 0.6 wt% h-BNNSs and 0.6 wt% m-BNNSs is calculated, according to Eq. (1). Under the testing conditions used, the MWV of the ball lubricated by LP without any additives is $3.33 \times 10^{-3}$ mm$^3$ (Fig. 6). The MWV of three additives are significantly decreased than that of LP, and they are $2.45 \times 10^{-3}$ mm$^3$, $1.88 \times 10^{-3}$ mm$^3$, $1.54 \times 10^{-3}$ mm$^3$, respectively. The results further show that three additives have significant anti-wear effects, suggesting that three additives deposit on sliding interfaces and form the tribo-films under contact stress. The tribo-films can remarkably reduce friction and avoid wear of steel balls caused by direct contact. As expected, h-BNNSs and m-BNNSs show a better wear-resistant effect than h-BN. Furthermore, m-BNNSs composite possesses the smallest MWV, which is decreased by as high as 53.8%.

Figure 7 shows the optical images of worn area lubricated with LP and LP containing different additives. The wear spots on steel ball can be observed very intuitively. The worn surface on steel ball lubricated by LP alone (Fig. 7a) shows severe wear with deep scratches and grooves. When lubricated by LP containing 0.6 wt% h-BN (Fig. 7b), h-BNNSs (Fig. 7c) and m-BNNSs (Fig. 7d),

**Fig. 7** Optical microscopy images of worn surfaces of steel balls: LP (**a**) and LP with 0.6 wt% h-BN (**b**), 0.6 wt% h-BNNSs (**c**), and 0.6 wt% m-BNNSs (**d**)
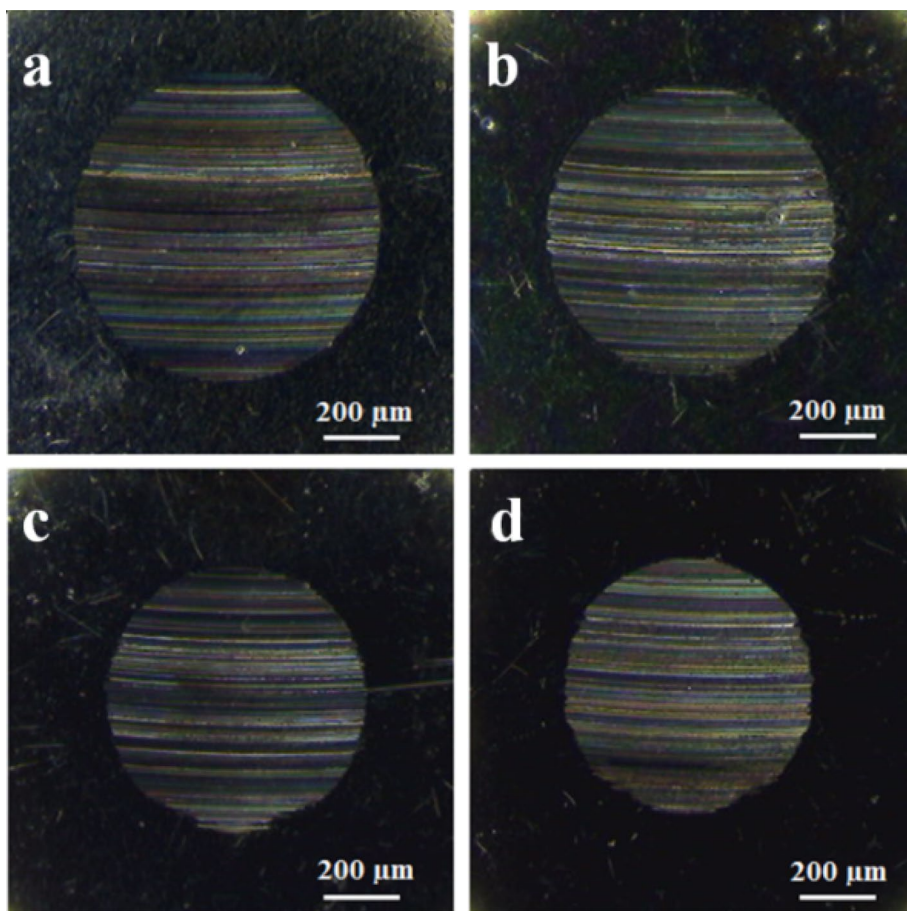


the surface of steel ball has been significantly improved and the size of wear scar is smaller than that of LP. Compared with h-BN and h-BNNSs, there are only some shallow and narrow scratches on steel ball lubricated by 0.6 wt% m-BNNSs, and the smallest wear scar are observed. The improvement order of three additives on the surface of steel ball obtained from Fig. 7 corresponds to the results of anti-wear property of three additives (Fig. 6).

Tribological test results show that m-BNNSs possesses more outstanding lubrication behaviors compared with h-BN or h-BNNSs. For m-BNNSs composite, the weak van der Waals interactions between layers provide low shear resistance under friction stress, thus reducing friction. In addition, m-BNNSs can effectively fill the wear area of the steel ball, and provide continuous protective films on rubbing surfaces, because of its excellent dispersion stability in LP, prevent direct contact of friction pairs, and further improve wear-resistance performance.

In order to prove that functionalized modification of h-BNNSs can significantly improve the tribological properties, we also compare m-BNNSs composite with the physical mixed additive h-BNNSs + KH570. As shown in Fig. 8, the anti-wear effect of h-BNNSs + KH570 is similar to that lubricated with LP containing 0.6 wt%

**Fig. 8** (**a**) Comparison of the average COFSs and average WSD for LP containing 0.6 wt% m-BNNSs and 0.6 wt% h-BNNSs + KH570. (**b**) The COF curves of pure LP, 0.6 wt% m-BNNSs/LP, and 0.6 wt% h-BNNSs + KH570/LP dispersions
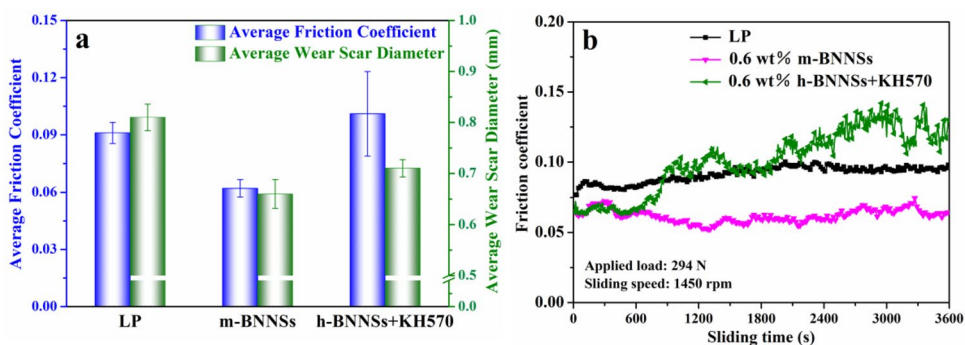
h-BNNSs (Fig. 6). Regrettably, 0.6 wt% h-BNNSs + KH570 dispersion possesses large COF, and the average COF value is tested to be 0.101, which is 11.0% higher than that of the LP (0.091). It should be explained that this is the result of a relationship between silane and LP can be caused. In contrast, the obtained m-BNNSs is much better of lubricating oil additive with superior properties in both fiction-reducing and anti-wear properties, which reflects its wide practical importance. As seen in Fig. 8b, the curve of 0.6 wt% m-BNNSs lower the curve of LP and 0.6 wt% h-BNNSs + KH570 during the whole test. For h-BNNSs + KH570, the COF values are smaller than LP before about 600 s due to the intrinsic tribological performances of h-BNNSs. Then the COF values of h-BNNSs + KH570 gradually increase from 600 to 900 s and finally close to the COF values of LP. As friction test continues, the COF curve of h-BNNSs + KH570 is above that of LP. This may be due to the fact that the non-covalent bond combination of KH570 and h-BNNSs will affect the dispersion of h-BNNSs in LP, and its tribological performance will be seriously deteriorated. These results further demonstrate that chemical functionalization h-BNNS by surface modifier containing lipophilic groups can significantly improve its dispersion and tribological behaviors in base oils.

## 4 Conclusions

In summary, m-BNNSs composite is synthesized by covalent interaction with silane coupling agent KH570 and h-BNNSs. The m-BNNSs composite has excellent dispersion stability in LP. Compared with h-BNNSs + KH570 prepared by physical blending method, m-BNNSs composite possesses better friction-reducing and wear resistance effects. Therefore, this facile and scalable reaction method of h-BNNSs opens up a new way for the potential application of h-BN in lubricant systems.

## Compliance with Ethical Standards

## References

1. Falin A, Cai Q, Santos E, Scullion D, Qian D, Zhang R, Yang Z, Huang K, Watanabe K, Taniguchi T, Barnett M, Chen Y (2017) Mechanical properties of atomically thin boron nitride and the role of interlayer interactions. Nat Common 8:15815

2. Cai Q, Du A, Gao G, Mateti S, Cowie B, Qian D, Zhang S, Lu Y, Fu L (2016) 2d nanomaterials: molecule-induced conformational change in boron nitride nanosheets with enhanced surface adsorption. Adv Funct Mater 26:8356–8356

3. Deepika LL, Glushenkov A, Hait S, Hodgson CY (2014) High-efficient production of boron nitride nanosheets via an optimized ball milling process for lubrication in oil. Sci Rep 4:7288

4. Shen B, Zhang T, Yin Y, Zhu Z, Lu L, Ma C, Zhou F, Yao H (2019) Chemically exfoliated boron nitride nanosheets form robust interfacial layers for stable solid-state Li metal batteries. Chem Commun 55:7703–7706

5. Nascimento R, Moraes E, Matos M, Prendergast D, Manhabosco T, de Oliveira A, Chacham H, Batista R (2019) Graphene/h-BN in-plane heterostructures: stability and electronic and transport properties. J Phys Chem C 123:18600–18608

6. Song Q, Fang Y, Wang J, Liang J, Hu Q, Liu Z, Huang Y, Xue Y, Lin J, Tang C (2019) Enhanced adsorption of fluoride on Al-modified boron nitride nanosheets from aqueous solution. J Alloys Compd 793:512–518

7. Xiong J, Di J, Zhu W, Li H (2020) Hexagonal boron nitride adsorbent: synthesis, performance tailoring and applications. J Energy Chem 40:99–111

8. Chen W, Shi H, Xin H, He N, Yang W, Gao H (2018) Friction and wear properties of $Si_3N_4$-hBN ceramic composites using different synthetic lubricants. Ceram Int 44:16799–16808

9. Hamidinejad M, Zandieh A, Lee J, Papillon J, Zhao B, Moghimian N, Maire E, Filleter T, Park C (2019) Insight into the directional thermal transport of hexagonal boron nitride composites. ACS Appl Mater Interfaces 11:41726–41735

10. Madhukar P, Selvaraj N, Rao C, Veeresh Kumar G (2019) Tribological behavior of ultrasonic assisted double stir casted novel nano-composite material (AA7150-hBN) using Taguchi technique. Compos B 175:107136

11. Berman D, Erdemir A, Sumant A (2018) Approaches for achieving superlubricity in two-dimensional materials. ACS Nano 12:2122–2137

12. Zhang R, Ding Q, Zhang S, Niu Q, Ye J, Hu L (2019) Construction of a continuously layered structure of h-BN nanosheets in the liquid phase via sonication-induced gelation to achieve low friction and wear. Nanoscale 11:12553–12562

13. Reeves C, Menezes P (2016) Evaluation of boron nitride particles on the tribological performance of avocado and canola oil for energy conservation and sustainability. Int J Adv Manuf Tech 89:3475–3486

14. Bondarev A, Kovalskii A, Firestein K, Loginov P, Sidorenko D, Shvindina N, Sukhorukova I, Shtansky D (2018) Hollow spherical and nanosheet-base BN nanoparticles as perspective additives to oil lubricants: correlation between large-scale

friction behavior and in situ TEM compression testing. Ceram Int 44:6801–6809

15. Yoo S, Park Y, Park C, Ryu H, Hong S (2018) Biomimetic artificial nacre: boron nitride nanosheets/gelatin nanocomposites for biomedical applications. Adv Funct Mater 28:1805948

16. Guo F, Yang P, Pan Z, Cao X, Xie Z, Wang X (2017) Carbon-doped BN nanosheets for the oxidative dehydrogenation of ethylbenzene. Angew Chem Int Ed Engl 56:8231–8235

17. Andriani Y, Song J, Lim P, Seng D, Lai D, Teo S, Kong J, Wang X, Zhang X, Liu S (2019) Green and efficient production of boron nitride nanosheets via oxygen doping-facilitated liquid exfoliation. Ceram Int 45:4909–4917

18. An L, Yu Y, Bai C, Bai Y, Zhang B, Gao K, Wang X, Lai Z, Zhang J (2019) Simultaneous production and functionalization of hexagonal boron nitride nanosheets by solvent-free mechanical exfoliation for superlubricant water-based lubricant additives npj 2D Mater. Appl 3:28

19. E S, Zhang X, Li C, Long X, Li Z, Ma S, Li Q, Geng R, Lu W, Yao Y, (2018) Tribological characteristics of boron nitride nanosheets on silicon wafers obtained by the reaction of $MgB_2$ and $NH_3$. Surf Coat Technol 340:36–44

20. Sahu J, Panda K, Gupta B, Kumar N, Manojkumar P, Kamruddin M (2018) Enhanced tribo-chemical properties of oxygen functionalized mechanically exfoliated hexagonal boron nitride nanolubricant additives. Mater Chem Phys 207:412–422

21. Ma Z, Ding H, Liu Z, Cheng Z (2019) Preparation and tribological properties of hydrothermally exfoliated ultrathin hexagonal boron nitride nanosheets (BNNSs) in mixed NaOH/KOH solution. J Alloys Compd 784:807–815

22. Ahmad P, Khandaker M, Amin Y, Amin M, Irshad M, Din I (2015) Low temperature synthesis of high quality BNNTs via argon supported thermal CVD. Ceram Int 41:15222–15226

23. Wang Y, Wan Z, Lu L, Zhang Z, Tang Y (2018) Friction and wear mechanisms of castor oil with addition of hexagonal boron nitride nanoparticles. Tribol Int 124:10–22

24. Kumari S, Sharma O, Gusain R, Mungse H, Kukrety A, Kumar N, Sugimura H, Khatri O (2015) Alkyl-chain-grafted hexagonal boron nitride nanoplatelets as oil-dispersible additives for friction and wear reduction. ACS Appl Mater Interfaces 7:3708–3716

25. Weng Q, Wang X, Wang X, Bando Y, Golberg D (2016) Functionalized hexagonal boron nitride nanomaterials: emerging properties and applications. Chem Soc Rev 45:3989–4012

26. Mi Y, Gou J, Liu L, Ge X, Wan H, Liu Q (2019) Enhanced breakdown strength and thermal conductivity of BN/EP nanocomposites with bipolar nanosecond pulse DBD plasma modified BNNSs. Nanomaterials 9:1396

27. Yuan F, Jiao W, Yang F, Liu W, Xu Z, Wang R (2017) Surface modification and magnetic alignment of hexagonal boron nitride nanosheets for highly thermally conductive composites. RSC Adv 7:43380–43389

28. Wang L, Han W, Ge C, Zhang R, Bai Y, Zhang X (2019) Covalent functionalized boron nitride nanosheets as efficient lubricant oil additives. Adv Mater Interfaces 6:1901172

29. Han W, Ge C, Zhang R, Zhang X (2019) Synthesis of boron nitride microrods with fish-scale-like structures for enhanced thermal conductivity of water. Int J Heat Mass Transfer 132:1284–1295

30. Bai Y, Wang L, Ge C, Liu R, Guan H, Zhang X (2020) Atomically thin hydroxylation boron nitride nanosheets for excellent water-based lubricant additives. J Am Ceram Soc 103:6951–6960

31. Zhao L, Cai T, Ye M, Liu D, Liu S (2019) The regulation of the microstructure, luminescence and lubricity of multi-element doped carbon nanodots with alkylated diquaternary 1, 4-Diaz-abicyclo[2.2.2]octane derived dicationic ionic liquids inserted in carbon skeleton. Carbon 150:319–333

32. Chao Y, Liu M, Pang J, Wu P, Jin Y, Li X, Luo J, Xiong J, Li H, Zhu W (2019) Gas-assisted exfoliation of boron nitride nanosheets enhancing adsorption performance. Ceram Int 45:18838–18843

33. Bai Y, Han W, Ge C, Liu R, Zhang R, Wang L, Zhang X (2019) High thermal conductivity nanocomposites based on conductive polyaniline nanowire arrays on boron nitride. Macromol Mater Eng 304:1900442

34. Ruiz V, Yate L, Langer J, Kosta I, Grande H, Tena-Zaera R (2019) PEGylated carbon black as lubricant nanoadditive with enhanced dispersion stability and tribological performance. Tribol Int 137:228–235

35. Cheng Z, Ma Z, Ding H, Liu Z (2019) Environmentally friendly, scalable exfoliation for few-layered hexagonal boron nitride nanosheets (BNNSs) by multi-time thermal expansion based on released gases. J Mater Chem C 7:14701–14708

36. Cai W, Mu X, Pan Y, Guo W, Wang J, Yuan B, Feng X, Tai Q, Hu Y (2018) Facile fabrication of organically modified boron nitride nanosheets and its effect on the thermal stability, flame retardant, and mechanical properties of thermoplastic polyurethane. Polym Adv Technol 29:2545–2552

37. Cai Q, Scullion D, Falin A, Watanabe K, Taniguchi T, Chen Y, Santos E, Li L (2017) Raman signature and phonon dispersion of atomically thin boron nitride. Nanoscale 9:3059–3067

38. Li X, Hao X, Zhao M, Wu Y, Yang J, Tian Y, Qian G (2013) Exfoliation of hexagonal boron nitride by molten hydroxides. Adv Mater 25:2200–2204

39. Yurdakul H, Göncü Y, Durukan O, Akay A, Seyhan T, Ay N, Turtan S (2012) Nanoscopic characterization of two-dimensional (2D) boron nitridenanosheets (BNNSs) produced by microfluidization. Ceram Int 38:2187–2193

40. Kuang W, Zhao B, Yang C, Ding W (2020) Effects of h-BN particles on the microstructure and tribological property of self-lubrication CBN abrasive composites. Ceram Int 46:2457–2464

41. E S, Ye X, Zhu Z, Lu W, Li C, Yao Y (2020) Tuning the structures of boron nitride nanosheets by template synthesis and their application as lubrication additives in water. Appl Surf Sci 479:119–127

**Publisher's Note** Springer Nature remains neutral with regard to jurisdictional claims in published maps and institutional affiliations.